

# PENETRATION DEPTH OF BUBBLE SWARM ENTRAINED BY A PLUNGING WATER JET

MINORU KUMAGAI<sup>\*1)</sup>, HIROYUKI ISHIZAKI<sup>\*2)</sup>  
AND KAZUO ENDOH<sup>\*3)</sup>

Department of Chemical Process Engineering,  
Hokkaido University, Sapporo 060

**Key Words:** Chemical Reactor, Plunging Water Jet, Penetration Depth, Gas Entrainment, Bubble Swarm

## Introduction

When a liquid jet plunges into a liquid, a submerged two-phase region like a cone is formed in the liquid. The penetration depth of the bubble swarm is one of the important parameters for the design of plunging jet absorbers. Several experimental correlations with respect to penetration depth have already been established by some other workers, such as Suciu and Smigelschi<sup>7)</sup>, Van de Donk<sup>8)</sup> and McKeogh and Ervine<sup>5)</sup>. Their equations were, however, based only on the term regarding the momentum of a jet. It is obvious from our investigations<sup>2-4)</sup> that the penetration depth depends not only on the jet momentum but also on jet length, nozzle diameter and jet discharge angle. Taking into account these parameter dependences, this study proposes an experimental correlation for penetration depth in a wider range of application. Some comparisons between our and other workers' results are also made.

## 1. Experimental

Figure 1 shows the arrangement of the experimental apparatus. Gas entrainment occurs at the impinging point of a water jet on the water surface. The diameter of the primary bubbles is of the order of  $2 \times 10^{-5} - 10^{-4}$  m for an air-water system<sup>7)</sup> and of the order of  $2 \times 10^{-4}$  m for an air-liquid system<sup>1)</sup>. The bubble penetration depth ( $L_d$ ) is defined as the distance between the deepest point of bubble swarm and the water surface. Jet length ( $L_j$ ) and jet discharge angle ( $\alpha$ ) are also indicated in this figure. Nozzle inner diameters ranged from  $2.00 \times 10^{-3}$  to  $8.04 \times 10^{-3}$  m.  $L_j$  was in the range of 0.06-0.80 m.

## 2. Results and Discussion

Typical experimental results are given in Fig. 2. In this figure,  $L_d$  values are plotted against  $DV$  on a log-log

graph. The product of  $D$  and  $V$  represents the term concerning the momentum of a jet. The plot of  $L_d$  vs.  $DV$  is linear. The slope of each line changes with experimental conditions. In general,  $L_d$  decreases with increasing  $L_j/D$  ratio, and the dependence of  $L_d$  on  $DV$  decreases as  $L_j/D$  ratio is increased. The  $L_j/D$  ratio stands for the shape of a jet<sup>6)</sup>. These tendencies can be considered to be explained as follows. At the penetration depth, the vertical downward component of drag force acting on a bubble, which is exerted by jet flow, equals the buoyant force acting on it. Therefore, the bubble diameter is important and depends greatly on the bubble coalescence. The frequency of bubble coalescence can be affected by the gas entrainment rate ( $G$ ). The gas entrainment rate increased with the  $L_j/D$  ratio<sup>2,4)</sup>. It can be considered from this fact that an increase in the  $L_j/D$  ratio results in increasing frequency of bubble coalescence, i.e. bubble diameter, at constant  $D$ . In the case of long jets at constant  $D$ , the bubble swarm cannot penetrate appreciably because of the particularly large gas entrainment rate<sup>2)</sup>.

Data points, at  $D = 5.75 \times 10^{-3}$  m,  $L_j = 0.06$  m and  $\alpha = 60.0^\circ$ , deviate from the linear relationship at velocities lower than about  $V = 4$  m/s. It is interesting to examine the relation between this velocity and the gas entrainment curve, which is defined as a log-log plot of gas entrainment rate vs. jet velocity and can be divided into four regions by three critical jet velocities  $V_1^*$ ,  $V_2^*$  and  $V_3^*$ <sup>2-4)</sup>. The gas entrainment behaviors in regions I-IV are as follows<sup>3)</sup>: (I) intermittent entrainment with bubbles, (II) intermittent entrainment with relatively large bubbles, (III) the stage from discontinuous to continuous entrainment with bubble swarm and (IV) continuous entrainment with bubble swarm.  $V_2^*$  between regions II and III can be calculated from Eq. (1)<sup>2)</sup> and is about 3.2 m/s under the same experimental conditions as those in Fig. 2:  $D = 5.75 \times 10^{-3}$  m,  $L_j = 0.06$  m,  $v = 1.006 \times 10^{-6}$  m<sup>2</sup>/s (water at 20°C) and  $\alpha = 60.0^\circ$ .

$$V_2^* = 2.15 \times 10^6 v (L_j/D)^{0.15} \sin^{-0.3} \alpha \quad (1)$$

$V_2^*$  almost corresponds to the velocity at which the log-log plots of  $L_d$  against  $DV$  deviate from the linear rela-

<sup>\*1)</sup> Received April 11, 1992. Correspondence concerning this article should be addressed to M. Kumagai.

<sup>\*2)</sup> H. Ishizaki is now at Japan Metals and chem. Co., LTD., Takizawa 020-01.

<sup>\*3)</sup> K. Endoh is now at Hokkaido Information Univ., Ebetsu 069.

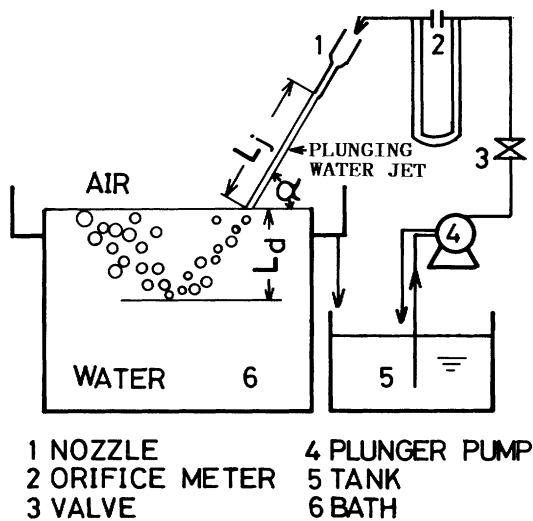


Fig. 1 Experimental apparatus

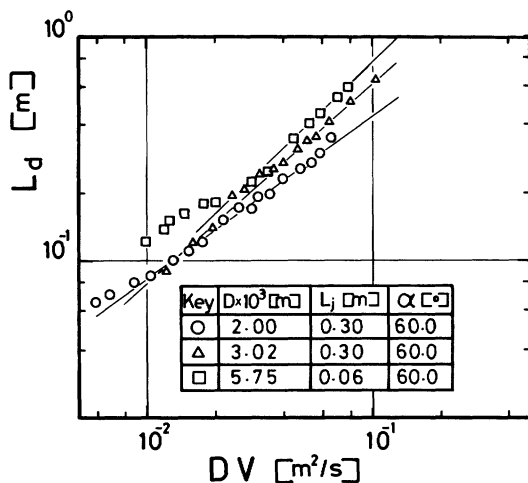


Fig. 2 Plots of  $L_d$  vs.  $DV$

relationship. Relatively large gas bubble entrainment takes place in the range of velocities lower than  $V_2^{*3}$ . Hence data points, which lie on a straight line and are greater than  $V_2^*$ , are used to establish an empirical correlation.

The slope of the straight line for the log-log plots of  $L_d$  vs.  $DV$  decreased with increasing  $L_j/D$  ratio. A lowering of the momentum dependency can be noticed. The  $L_j/D$  ratio, consequently, has an influence on an exponent of the term  $DV$ . In Fig. 3 the value of the slope of each straight line is indicated by the letter  $A$  and is plotted against the  $L_j/D$  ratio. Values of  $A$  are inversely proportional to one-sixth of the  $L_j/D$  ratio. On the other hand, the effects of the  $L_j/D$  ratio and jet discharge angle on  $L_d$  were experimentally found to be as follows:  $L_d \propto (L_j/D)^{-0.55}$  and  $L_d \propto \sin^{1.5} \alpha$ .  $L_d$  is correlated in Fig. 4 with the parameter group obtained by combining the above dependences. Data points fall on each straight line. Very good agreement with experimental data is found. The next equation is derived from this figure.

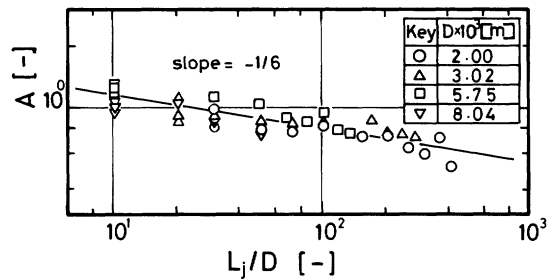


Fig. 3 Dependence of  $A$  on  $L_j/D$  ratio

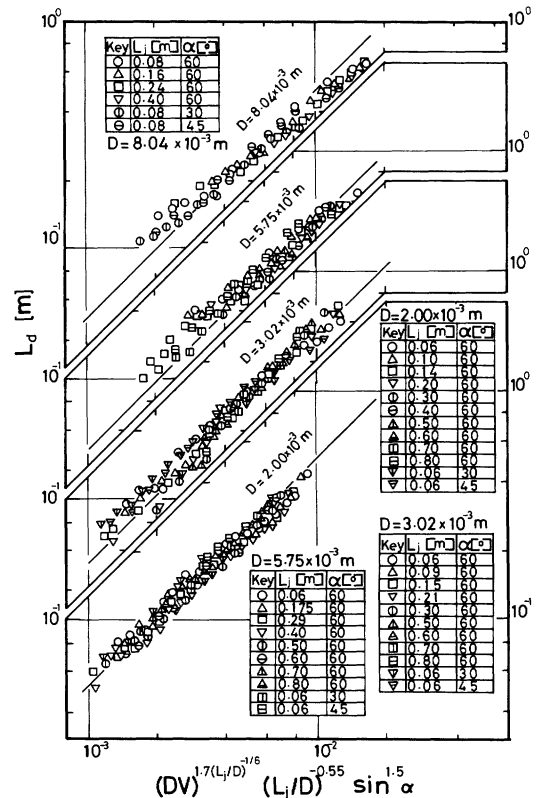


Fig. 4 Correlation of penetration depth ( $L_d$ ) with experimental conditions

$$L_d = 50 (DV)^A (L_j/D)^{-0.55} \sin^{1.5} \alpha \quad (2)$$

$$A = 1.7 (L_j/D)^{-1/6}$$

$$V: V_2^* - 34 \text{ m/s}, D: 2.00 \times 10^{-3} - 8.04 \times 10^{-3} \text{ m}, \\ L_j/D: 10 - 400$$

$L_d$  can be expressed as a function of three terms:  $DV$ ,  $L_j/D$  and  $\sin \alpha$ .

The following three relationships concerning penetration depth are available in the literature<sup>5, 7, 8</sup>.

$$\text{Suciu and Smigelschi}^7): L_d = 10 (DV) \quad (3)$$

$$V: 2.2 - 9.7 \text{ m/s},$$

$$D: 1 \times 10^{-3} - 4 \times 10^{-3} \text{ m}, L_j/D > 20$$

$$\text{Van de Donk}^8): L_d = 2.4 (DV)^{0.66} \quad (4)$$

$$V: 3 - 13 \text{ m/s},$$

$$D: 4 \times 10^{-3} - 1 \times 10^{-1} \text{ m}, L_j/D: 3.5 - 50$$

$$\text{McKeogh and Ervine}^5): L_d = 2.6 (DV)^{0.7} \quad (5)$$

$$V: 1 - 7 \text{ m/s}, D: 6 \times 10^{-3} - 3 \times 10^{-2} \text{ m},$$

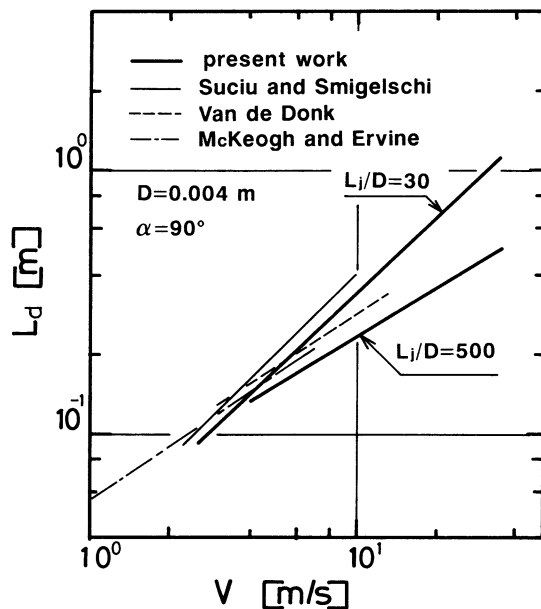


Fig. 5 Comparison of calculated values from present equation with those from other authors' equations

$L_j$  = jet disintegration length

The above three equations are established as a function of  $DV$  only. Jet length effect is neglected in both Eq. (3) and Eq. (4). Jet length is almost equal to jet disintegration length in Eq. (5). **Figure 5** represents a comparison between our equation and those of other workers at  $D = 4 \times 10^{-3}$  m and  $\alpha = 90^\circ$ . The two solid lines give the calculated values from Eq. (2) for  $L_j/D = 30$  and 500. Equation (5) for long jets fits in with Eq. (2) in the case of  $L_j/D = 500$ . Equation (3), presented in the range of  $L_j/D = 20-40$ , tends to coincide with Eq. (2) for  $L_j/D =$

30. The discrepancy is about 15%. The difference among calculated values from Eqs. (3), (4) and (5) is caused by the effect of the  $L_j/D$  ratio. The  $L_j/D$  ratio dependency becomes more appreciable at high velocities. No other equation for high velocities has been presented. It is found that Eq. (2) can be employed to estimate  $L_d$  in a wider range of operating conditions, especially at high jet velocities and at different  $L_j/D$  ratios.

#### Nomenclature

$A$	= exponent of $DV$	
$D$	= nozzle inner diameter	[m]
$G$	= gas entrainment rate	[m <sup>3</sup> /s]
$L_d$	= penetration depth of bubble swarm	[m]
$L_j$	= jet length	[m]
$V$	= water jet velocity at nozzle exit	[m/s]
$V_1^*, V_2^*, V_3^*$	= critical jet velocity on the gas entrainment curve	[m/s]
$\alpha$	= jet discharge angle	[°]
$\nu$	= kinematic viscosity	[m <sup>2</sup> /s]

#### Literature Cited

- 1) Hara, H., K. Shimada, M. Kumagai and K. Endoh: *Kagaku Kogaku Ronbunshu*, **3**, 424-425 (1977)
- 2) Kumagai, M. and H. Imai: *Kagaku Kogaku Ronbunshu*, **8**, 1-6 (1982)
- 3) Kumagai, M. and H. Imai: *Kagaku Kogaku Ronbunshu*, **8**, 510-513 (1982)
- 4) Kumagai, M. and K. Endoh: *J. Chem. Eng. Japan*, **15**, 427-433 (1982)
- 5) McKeogh, E.J. and D.A. Ervine: *Chem. Eng. Sci.*, **36**, 1161-1172 (1981)
- 6) Ohyama, Y., Y. Takashima and H. Idemura: *Kagaku Kenkyusho Hokoku*, **29**, 344-348 (1953)
- 7) Suciu, G. D. and O. Smigelschi: *Chem. Eng. Sci.*, **31**, 1217-1220 (1976)
- 8) Van de Donk, J.: Ph. D. Thesis, Delft, 91-93 (1981)